Molecular docking analysis of chemical constituents from the stem barks of podocarpus falcatus and evaluation for antibacterial activity

Desalegn Abebe Deresa (desalegnabebe37@gmail.com)
Wollega University
Zelalem Abdissa
Wollega University
Getahun Tadesse. Gurmessa
Wollega University
Negera Abdissa
Jimma University

Article

Keywords: Podocarpus falcatus, 4β-carboxy-19-nor-totarol, β-sitosterol, p-hydroxybenzoic acid, methyl-3, 4, 5-trimethylhex-2-enoate, antibacterial activity, molecular docking, ADMET

Posted Date: April 13th, 2022

DOI: https://doi.org/10.21203/rs.3.rs-1505415/v1

Abstract

Chromatographic separation of equal ratio of CH_2Cl_2-MeOH extract of the stem barks of *Podocarpus falcatus* led to the isolation of three compounds namely: 4*β*-carboxy-19-nor-totarol (**1**), β-sitosterol (**2**), 4-hydroxybenzoic acid (**3**) and (E)-methyl-3, 4, 5-trimethylhex-2-enoate (**4**). The structures of the compounds were established based on the analysis of 1D and 2D NMR spectroscopic data. These compounds were reported from this plant for the first time. The crude extract and isolated compounds were evaluated for their antibacterial activity using disk diffusion assay method. The crude extract showed a strong activity against *S. aureus*. Compounds (**1**) and (**2**) showed a relatively moderate activity against *S. flexineri* and *S. typhimurium* respectively, whereas, compound (**3**) and (**4**) demonstrated a strong activity against *S. aureus*. The crude extract and the isolated compounds showed considerable antibacterial activity as compared to the reference *gentamycin* indicating that this plant has potentially antibacterial properties. Docking studies were performed with *S. aureus* Gyrase and human DNA topoisomerase IIβ by using AutoDock Vina. ADMET were predicted by Swiss ADME, Pre ADMET. In silico, molecular docking studies of compounds (**1-3**) showed strong interaction with *S. aureus* Gyrase with binding energy value ranging from −6.1 to −8.6 kcal/mol, with respect to ciprofloxacin and Doxycycline −8.4 kcal/mol and -13.0 kcal/mol respectively, whereas, analysis against human topoisomerase IIβ with binding energy value ranging from −6.4 to −10.1 kcal/mol, with respect to Vosaroxin and Abiraterone −10.2 and -11.8 kcal/mol respectively. The results obtained suggest that compounds (**1-3**) are potential *S. aureus* Gyrase inhibitors and might be used as antibacterial agents and compound (**1** and **2**) are potential topoisomerase IIβ inhibitors and might be used as anticancer agents. The ADMET studies showed the highest drug-likeness properties for studied compounds (**1-3**). Compounds (**1-3**) have no acute toxicity. The studied compounds were predicted to be non- hepatotoxic, non-cytotoxic, non-mutagenic and non-irritant. However, compound (**2**) is Immunotoxic

1. Introduction

The *Podocarpus* (Podocarpaceae family) is one of the largest genera of the family consisting of about 94 species distributed from south temperate zones through the tropical highlands, West India and Japan [1]. Phytochemical and pharmacological studies of Podocarpus genus led to the isolation of a number of bioactive diterpenes, including nor- and bisnor- diterpenoid lactones [2]. In addition, totarane-type diterpenes such as totarol and their dimers (macrophyllic acid) have also been reported from many species of *Podocarpus*, These compounds were considered to be chemical markers of the genus [3]. *Podocarpus falcatus* (Thunb.) is belongs to with the vernacular name zigiba. It is an evergreen, dioecious, medium to large-sized tree up to 60m tall widely distributed in Ethiopia, Kenya, Tanzania, Mozambique, South Africa, and Madagascar [1], [2]. Besides its commercial and ecological importance, it has also known for its ethnobotanical values in Ethiopia. The roots of this plant were used as anticancer remedies [4, 5]. Crushed and juice of the leaves were taken for vomiting, where as the root dried powdered, mixed with water were taken for febrile illness. Decoction of the fruit serves as a tonic for cleaning the kidneys, lungs and stomach [6]. Despite of the wider use of this plant by the communities for medicinal purposes, the phytochemical and bioactivity information pertaining to the stem bark of this plant is limited. Therefore, as part of the search for new bioactive molecules from Ethiopian medicinal plants, the isolation of five compounds and antibacterial activities of the extract and the compounds were reported here.

2. Materials And Methods

2.1. General Method

Solvents and reagents used for extraction and purification of the compounds are of analytical and HPLC grade. Analytical TLC pre-coated sheets ALUGRAM®Xtra SIL G/UV_{254} (layer: 0.20mm silica gel 60 with fluorescent indicator $UV_{F254/365}$) was used for purity analysis. For column chromatography, silica gel 100–200 mesh was used. Chromatograms were visualized on TLC by spraying with 10% H_2SO_4 and heating on hot plate. NMR spectra data were recorded on an Avance 600 MHz spectrometer (Bruker, Billerica, MA, USA, at 600MHz (^1H) and 150MHz (^{13}C). Chemical shifts were expressed in parts per million (ppm) downfield of Trimethylsilane (TMS) as internal reference for ^1H resonances, and referenced to the central peak of the appropriate duetrated solvent's resonances (residual $CDCl_3$, $(CD_3)_2CO$, MeOD and $(CD_3)_2SO$ at δ_H7.26, 2.20, 3.35, 2.52 for protons and δ_C79.16, 205.87, 49.77, 40.76 for carbons respectively).Whatman filter paper No.3, DMSO, Petri dishes and gentamycin were used in antibacterial analysis.

2.2. Plant materials

The stem bark of *P. falcatus* was collected from Horro Buluk, Horro Guduru Wollega zone, Oromia regional state, Ethiopia in September, 2020. The plant material was identified by botanist (Dr. Fekadu Gurmessa) and the voucher specimen (DAD002Pf) has been deposited

in Wollega University Herbarium. The collected plant part was washed thoroughly with tap water and cut into smaller pieces and dried under shade.

2.3. Extraction and isolation

The powdered stem bark of *P. falcatus* (850 g) was extracted with equal ratio of CH_2Cl_2-MeOH (3x3L) at room temperature for 48 hr each with occasional shaking. The crude extract was filtered from marc using Whatman filter paper. The solvent was evaporated under reduced pressure using rotary evaporator at 40^0C to yield (20 g, 2.7%) of dark brown crude extract. About 18 g of the extract was adsorbed on 25 g of silica gel and subjected to column chromatography, packed with silica gel (320 g). The column was eluted with hexane with increasing gradient of ethyl acetate to afford 30 major fractions *ca*. 100 mL each. Fractions with similar TLC profiles were combined together for further purification. Fractions 6–10 (2% EtOAc in hexane) were combined together 20 mg and refined by Sephadex LH-20 (eluting with CH_2Cl_2/MeOH; 1:1) afforded (**1**, 15 mg) while fractions15-20 (3% EtOAc in hexane) showed similar TLC profiles were combined together gave 18 mg and purified by washing with excess petroleum ether gave compound (**2**, 12 mg). Fractions 26–30 (6% EtOAc in hexane) showed similar spots combined together afforded 15 mg and purified further by Sephadex LH-20 (eluting with CH_2Cl_2/MeOH; 1:1) afforded compound (**3**, 10 mg) and compound (**4**, 8 mg).

2.4. Antibacterial activity assay

Five pathogenic bacterial strains, one gram-positive (*Staphylococcus aureus* (ATCC25923)) and four gram-negative (*Escherichia coli* (ATCC25922), *Pseudomonas aeruginosa* (ATCC27853), *Salmonella typhimurium* (ATCC13311), and *Shigella flexneri* (ATCC29903) were obtained from the Department of Biology, Wollega University and used for evaluation of antibacterial activities. Antibacterial activities of the methanol extract and isolated compounds were tested against five bacterial strains using the disc diffusion method as described in [7] with slight modification. The test solutions were prepared with known weight of crude extract (0.01mg) and isolated compounds were dissolved in 1mL of DMSO. A 0.6 mm diameter sterile Whatman test disks were placed on the surface of the inoculated Mueller Hinton Agar in a 90 mm petridishes and then 0.01 mg/mL of the crude extract and the isolated compound (**1, 2, 3** and **4)** were applied onto the disks. Gentamicin (10 µg) and DMSO were used as the positive and negative controls respectively. The test samples were allowed to diffuse for 30 minutes and the plates were then kept in an incubator at 37°C for 24hr [8].The experiments were carried out in triplicate and the mean of the diameter of the inhibition zones were calculated. The antibacterial activity was determined by measuring the zone of growth inhibition surrounding the disks Antibacterial inhibition activities were measured against the standard.

2.5. In silico molecular docking Methodology

2.5.1. Preparation of ligands

The 2D structures (.mol) of all isolated compounds (**1–3**) were drawn and each individual structure was analyzed by using ChemDraw 16.0. The selected molecules were treated quantum mechanically by applying DFT method using the Gaussian 09 program suite at the Becke-3-Lee-YangPar (B3LYP) level combined with the standard 6-31G (d,p) basis set. During the optimization procedure, all the parameters were set in order to obtain a stable structure with minimum energy. The global minimum energy of the title compound was determined from the structure optimization procedure. The 3D coordinates (.PDB) of each molecule were obtained through the optimized structure.

2.5.2. Preparation of macromolecules

The crystal structure of receptor molecules *S. aureus* Gyrase (PDB ID 2XCT) and human topoisomerase IIβ with DNA (PDB ID 3QX3) were downloaded from protein data bank. The protein preparation was done using the reported standard protocol by removing the co-crystallized ligand, selected water molecules and cofactors, the target protein file was prepared by leaving the associated residue with protein by using Auto Preparation of target protein file Auto Dock 4.2.6 (MGL tools 1.5.6).

2.5.3. Autodock Vina analysis

The graphical user interface program Auto Dock 4.2.6 was used to set the grid box for docking simulations. The grid was set so that it surrounds the region of interest in the macromolecule. The docking algorithm provided with Auto Dock Vina was used to search for the best-docked conformation between ligand and protein. During the docking process, a maximum of nine conformers were considered for each ligand. The conformations with the most favorable (least) free binding energy were selected for analyzing the interactions between the target receptor and ligands by Discovery studio visualizer.

AutoDock Vina with the standard protocol was used to dock the protein S. aureus Gyrase (PDB ID 2XCT) and human topoisomerase IIβ with DNA (PDB ID 3QX3) and isolated ligands (**1–3**) into the active site of proteins. The molecular docking studies were carried out using Auto Dock Tools (ADT) [9]„ which is a free graphic user interface (GUI) for the AutoDock Vina program. The grid box was constructed using 20x20x20, pointing in x, y, and z directions, respectively, with a grid point spacing of 0.375 Å. The center grid box is of 62x30x62 Å for 2XCT and of 65x40x65 Å for 3QX3. Nine different conformations were generated for each ligand scored using AutoDock Vina functions and were ranked according to their binding energies. The ligands are represented in a different colour, H-bonds, and the interacting residues are represented in stick model representation.

3. Result And Discussion

The stem bark of *P. falcatus*was exhaustively extracted with equal ratio of CH_2Cl_2-MeOH solvent combination. The extract was subjected to column chromatography on silica gel followed by purification on Sephadex LH-20 and affordedfour compounds 1–4 (Fig. 1).

3.1. Characterization

Compound **1** was isolated as white powder with melting points of 175-177^{0}C. The^{1}HNMR spectrum showed 12 signals, with a highly downfield shifted proton signal at 12.07 assigned to carboxylic acidic proton whereas, proton signals at 6.96(1H, d, 8.6 Hz) and 6.41(1H, d, 8.6 Hz) assigned to *ortho*-coupled aromatic protons (H-11, H-12), two overlapped doublets at 1.33 (6H, d, 7.1 Hz) were an isopropyl moiety and the rest proton signals correspond to non-aromatic protons. ^{13}C NMR spectrum showed six aromatic carbon signals resonating at δ_C 149.5, 142.1, 134.6, 133.4, 126.6 and 113.4 assigned to C-13, C-9, C-14, C-8, C-11 and C-12 carbons, respectively(Table 1).

The remaining protons and carbons were assigned on the basis of 2D-NMR data, notably, HSQC and HMBC. The COSY spectrum showed coupling between H-2/H-3, H-5/H-6. The HSQC spectrum showed the presence of twelve signals suggested that compound **1** possesses four saturated methylene groups, although their respective proton signals could not be fully determined due to their significant overlapping. The HMBC correlations between methyl protons H-16 and H-17 with C-14 indicated that the isopropyl group is attached to the aromatic ring at C-14. Moreover, a cross peak in the HMBC spectrum between H-18 and δ_C at 178.9 ppm, confirmed the presence of a carboxylic acid group attached at C-4. Similarly, C-4 at δ_C 43.4 was assigned on the basis of a HMBC cross peak (Fig. 2) to H-18. The above evidence was in agreement with a totarane-type diterpenes skeleton and corresponded to the known compound 4*β*-carboxy-19-nortotarol, which matched with the reported data for this compound [10].

Table 1

^{1}H and ^{13}C NMR spectra data of compound (1)

Carbon No.	Appearance	^{13}C NMR	δH (int., mult., J in Hz)	HMBC
1	CH_2	40.5	2.53(1H,m),2.17(1H,m)	C-5, C-7, C-8, C-10
2	CH_2	20.4	1.51(1H,overlap),1.38(1H,m)	
3	CH_2	37.5	2.09(1H,overlap), 1.02(1H,m)	
4	C	43.4		
5	CH	51.7	1.41(1H,dd, 12.3,1.5 Hz)	
6	CH_2	21.5	2.18(1H,br dd, 12.3, 5.1 Hz) 2.16(1H,ddd, 12.3, 6.7,5.1,1.6 Hz)	C-5, C-7,C-8, C 10
7	CH_2	29.9	2.91(1H,dd, 16.7, 4.8 Hz) 2.60(1H,ddd,16.7, 12.4, 6.5 Hz)	C-5,C-6, C-8,C-9 C-5, C-8, C-9, C-10
8	C	133.4		
9	C	142.1		
10	C	38.5		
11	CH	126.6	6.96(1H,d, 8.6 Hz)	C-8, C-13
12	CH	113.4	6.41(1H,d, 8.6 Hz)	C-9, C-11
13	C	149.5		
14	C	134.6		
15	CH	28.8	3.17(1H,m)	
16	CH_3	20.6	1.33(3H,d, 7.1 Hz)	C-14, C-15,C-17
17	CH_3	21.1	1.33(3H,d, 7.1 Hz)	C-14, C-15,C-16
18	CH_3	21.2	1.23(3H,s,)	C-2, C-3, C-4, C-5, C19
19	C	178.9		
20	CH_3	23.7	1.06(3H,s)	C-1,C-5, C-9, C-10

Compound 2 was isolated as a white powder with melting points of 134 – 136^0C. The structure of this compound was identified to be β-sitosterol using ^{1}H and ^{13}C spectra data. The ^{1}H NMR spectrum showed an olefinic proton at δ_H 3.54(1H, tdd, 11.2, 6.5, 4.6 Hz) corresponds H-6 and oxymethine proton at δ_H 3.54(1H, tdd, 11.2, 6.5, 4.6 Hz) for H-3. It also showed proton signals at δ_H 0.69(3H, s), 1.02(3H, s), 0.94(3H,d, 6.5 Hz), 0.84(3H, d, 6.8 Hz), 0.81(3H, d, 6.8 Hz), 0.85(3H, t, 7.2 Hz) for six methyl groups and were assigned to H-18, H-19, H-21, H-26, H-27 and H-29, respectively.

The ^{13}C NMR spectrum showed signals for 29 carbon atoms including signals for six methyl (19.8, 19.4, 19.1, 18.8, 11.9 and 11.8), eleven methylene (δ_C 42.2, 39.8, 37.3, 33.9, 31.9, 31.6, 28.3, 26.1, 24.3, 23.1 and 21.1), nine methine (δ_C 121.7, 71.8, 56.8, 56.1, 50.1, 45.8, 36.2, 31.9 and 29.2) and three quaternary (δ_C 140.7, 42.3 and 36.5) carbon atoms. The recognizable signals at 140.9(C-5) and 121.9(C-6) are typical alkenes double bonds. The signals at δ 19.2 and 12.1 correspond to angular methyl carbon atoms(C-19) and (C-18) respectively (Table 2). Signal at 71.9 is assignable to the β-hydroxyl group attached to the carbon at (C-3). Therefore, based on these spectral datawhich is in agreement with existing literature reported for β-sitosterol [11].

Table 2

^{1}H and ^{13}C NMR spectra data of compound (2) and β-sitosterol

Carbon No.	Experimental ^{13}C NMR	^{1}H NMR	Literature ^{13}C NMR	^{1}H NMR	Appearance
1	37.4		37.28		CH_2
2	32.1		31.69		CH_2
3	71.9	3.54(tt, 1H)	71.82	3.53(m,1H)	CH
4	42.5		42.33		CH_2
5	140.9	-	140.70		C
6	121.9	5.37(dd,1H)	121.72	5.36(dd,1H)	CH
7	31.8		31.69		CH_2
8	32.1		31.93		CH
9	50.3		50.17		CH
10	36.7		36.52		C
11	21.2		21.10		CH_2
12	39.9		39.80		CH_2
13	42.5		42.33		C
14	56.2		56.79		CH
15	24.5		24.57		CH_2
16	28.4		28.25		CH_2
17	56.9		56.09		CH
18	12.1	0.70(s, 3H)	11.86	0.63(s, 3H)	CH_3
19	19.2	1.03(s, 3H)	19.40	1.01(s, 3H)	CH_3
20	36.3		32.52		CH
21	18.9	0.94(d, 3H)	18.79	0.93(s, 3H)	CH_3
22	34.1		33.98		CH_2
23	26.2		26.14		CH_2
24	45.9		45.88		CH
25	29.3		28.91		CH
26	19.9	0.84(3H, d, 6.4Hz)	19.80	0.84(s, 3H)	CH_3
27	19.6	0.88(3H, d, 6.4Hz)	18.79	0.83(s, 3H)	CH_3
28	23.2		23.10		CH_2
29	12.0	0.84(s, 3H)	11.99	0.81(s, 3H)	CH_3

Compound 3 was isolated as white amorphous with melting points of 214-215^{0}C. The ^{1}H-NMRspectrum showed fourproton signals.Signals atδ_H 7.78 (2H, d, 8.5Hz) assigned to two overlapping aromatic protons (H-2, H-6) and signal at 6.82(2H, d, 8.6Hz)

allocated to two overlapping protons (H-3, H-5). Whereas, proton signals at 12.41(1H; s) corresponds to carboxylic acid proton and signal at 10.22(1H, s) assigned to OH proton.

The ^{13}C NMR spectrum showed seven carbons signals corresponding to four aromatic methine at δ_C 131.9 assigned to two overlapping carbons (C-2, C-6) and at 115.6 assigned to two overlapping carbons (C-3, C-5), three quaternary, one for carboxylic acid at 167.6 (C-7),121.8 (C-1) and 162.1(C-4)(Table 3).The 2D experiment COSY and HSQC spectra of compound **3** allowed, respectively, the detection of the scalar couplings of the protons and connectivity of each proton to directly linked carbon atom. The COSY spectrum shows coupling between H-2/ H-3 and H-5/H-6.The HSQC shows two protonated carbons at 7.79(H-2 and H-6) linked with 131.9 (C-2 and C-6) and 6.82(H-3 and H-5) linked with 115.6 (C-3 and C-5). The HMBC spectrum reveals the correlation between the cross peak δ_H 7.79 (H-2and H-6) correlated with 115.6 (C-3and C-5), 131.9(C-4) and 167.6(C-7), proton at 6.82 (H-3 and H-5) correlated with 121.8(C-1), 115.6(C-3), 162.1(C-4) and proton at 10.22(OH proton) correlated with 115.6 (C-3 and C-5) and 162.1(C-4) that reveals the position of OH at C-4.Based on the basis of spectral analysis of 1D and 2D NMR compound **3** was identified as 4-hydroxybenzoic acid as shown in (Figure.3).

Compound **4** was isolated as white powdercompound. The $^{1}HNMR$ spectrum of the compound displayed one olefinic protonsat δ_H 8.11 (1H, s) assigned to (H-2), two saturated methines at 2.38 (1H, m, H-4) and 1.28(1H, m, H-5). The spectrum also showed three methyl protons at 1.32(3H, d, H-8), 1.26(3H, d, H-6/7), 0.90(3H, s, H-9) and one methoxy proton at 4.71(3H, s, H-10). The ^{13}C NMR showed a carbonyl resonance at δ_C 165.3 (C-1), olefinic carbons at 133.8(C-3), 129.7(C-2) and as well as five signals assignable at 62.8 (C-10), 33(C-4), 31(C-5), 29.7(C-6/7), 22.7(C-8) and 14.1(C-9) (Table 3). The DEPT spectrum showed three methine carbons at 129.7(C-2), 33(C-4), 31(C-5), four methyl carbons at 62.8(C-10), 29.7(C-6/7), 22.7(C-8) and 14.1(C-9). The COSY spectrum displayed three coupling protons H-4/H-8, H-4/H-5 and H-5/H-6/7. The HMBC spectrum showed the correlation between carbons and protons were shown on Fig. 4. Based on the spectroscopic data analysis, compound 4 was identified as (E)-methyl 3, 4, 5-trimethylhex-2-enoate.

Table 3

^{1}H and ^{13}C NMR spectra data for compound (3) and (4)

Compound 3			**Compound 4**				
Carbon No.	^{13}C NMR	δ_H(m, J in Hz)	Carbon No.	^{13}C NMR	δ_H(m, J in Hz)	Appearance	HMBC
1	121.8	-	1	165.3	-	C	-
2 & 6	131.9	7.79 (2H, d, 8.5 Hz)	2	129.7	8.11 (1H, s)	CH	C-1, C-3
3 & 5	115.6	6.82 (2H, d ,8.6 Hz)	3	133.8	-	C	
4	162.1	-	4	33.3	2.38 (1H, m)	CH	C-8
7	167.6	-	5	31.6	1.28(1H, m)	CH	C-6, C-7
			6	29.7	1.26(3H, d, 6.4 Hz)	CH_3	
			7	29.7	1.26(3H, d, 6.4 Hz)	CH_3	
			8	22.7	1.63(3H, d, 6.2 Hz)	CH_3	
			9	14.1	0.90(3H, s)	CH_3	C-4
			10	62.8	4.71(3H,s)	CH_3	C-1

3.2. Antibacterial activity result

The antibacterial activity of the crude extract and the isolated compounds were determined by the disk diffusion method against different bacteria. The bacterial strains were *E.coli, S. aureus, S. flexineri, S.typhimurium* and *P. aeruginosa*. The results of the diameters of inhibition zones are shown in (Table 4).

Table 4
Antibacterial activity test for crude and isolated compounds from *P. falcatus*

Crude extract/ compound	Bacteria inhibition zone (mm)				
	E.coli	*S. aureus*	*S. flexineri*	*S. typhimurium*	*P. aeruginosa*
PfME	10.03 ± 0.03	23.03 ± 0.05	19.07 ± 0.02	15.23 ± 0.21	13.13 ± 0.04
1	7.16 ± 0.24	7.33 ± 0.47	10.16 ± 0.24	7.33 ± 0.47	7.66 ± 0.24
2	8.00 ± 0.41	7.16 ± 0.24	8.16 ± 0.24	8.67 ± 0.47	8.33 ± 0.24
3	8.06 ± 0.09	22.13 ± 0.12	11.23 ± 0.33	9.22 ± 0.47	8.10 ± 0.08
4	8.36 ± 0.02	9.60 ± 0.22	7.10 ± 0.01	9.15 ± 0.20	7.25 ± 0.20
Gentamycin	22.13 ± 0.05	19.5 ± 0.04	20.03 ± 0.05	20.10 ± 0.03	14.06 ± 0.06
DMSO	-	-	-	-	-

The antibacterial activity test result showed varying degree of inhibition of the growth of bacterial strains. The crude extract showed considerable activity on both Gram-positive and Gram-negative bacterial strains with zone of inhibition ranging from 10.03 ± 0.03–23.03 ± 0.05 mm with the highest activity (23.03 ± 0.05 mm) was observed against *S. aureus*, which is even greater than that of the reference drug (gentamycin, 19.5 ± 0.04 mm) against the same strain Whereas, the isolated compounds showed moderate activities against all the test strains. This variation in inhibition of the bacterial growth by the crude extract and isolated compounds could be related to the synergetic effects of the various kinds of compounds present in the crude extracts or the minor compounds in the extract that could showed this activity have not been isolated. In general, the remarkable activities of the crude extract from this medicinal plant (*P. falcatus*) support the traditional use of the plant and could be used as a potential candidate in the development of novel antibacterial agents.

3.3. Molecular docking analysis

The results obtained from molecular docking study revealed that the isolated compounds (**1–3**) showed a strong binding affinity towards *S. aureus* Gyrase (PDB ID 2XCT) with binding energy value ranging from − 6.1 to − 8.6 kcal/mol, with respect to ciprofloxacin and Doxycycline − 8.4 and 13.0 kcal/ mol respectively (Table 5, Fig. 4). Compound (**1**) showed strong binding energy (− 8.6 kcal/mol) compared to ciprofloxacin − 8.4 kcal/mol and compound (**2** and **3)** good binding energy (-7.5, -6.1 kcal/mol) respectively compared to ciprofloxacin (− 8.4 kcal/mol). Compounds (**1** and **2**) showed one hydrogen bond interaction with active site of *S. aureus* Gyrase Arg-458 and Met-1121 respectively. Compound (**3)** showed five hydrogen bond interactions with (Arg-1122, DA-13, DG-9, Gly-1082, DT-8) protein residues. Hydrophobic interactions were observed for all isolated compounds (**1–3**) suggesting the compounds may act as inhibitors of *S. aureus* Gyrase. On the other hand, the isolated compounds (**1** and **2**) showed a strong binding affinity towards Human topoisomerase IIβ with binding energy value ranging from − 9.2 to − 10.1 kcal/mol, with respect to Vosaroxin − 10.2 kcal/ mol (Table 6, Fig. 5). Compound (**3**) showed weak binding energy ranging − 6.4 kcal/mol compared to Vosaroxin (− 10.2 kcal/mol). The results obtained suggest that compounds (**1** and **2)** are potential topoisomerase IIβ inhibitors and might be used as anticancer agents.

Table 5
Molecular docking results of isolated compounds against *S. aureus* Gyrase (PDB ID 2XCT)

Compound	Binding Affinity (kcal/mol)	H-bond	Residual interactions	
			Hydrophobic, Electrostatic & others	Van der Waals
1	− 8.6	Arg-458	Arg-458, DA-13 DG-9, Arg-458	DC-12, DA-11, DT-10
2	− 7.5	Met-1121	Ala-1120	Ser-1084, Met-1121, Asp-1083, DT-10, DG-9, DA-11, Arg-1122, Ala-1120
3	− 6.1	Arg-1122, DA-13, DG-9, Gly-1082, DT-8	DT-8	Ser-1084
Doxycycline	−13.0	Ser-438, Ser-1084, Ser-1084: HG, Ser-1084: Arg-1122: HH12, DG-9	Asp-1083, Ala-1120	Arg-1122, Met-1121, Phe-1123, Asp-437, DG-9, DT: G-10, DT: H-10
Ciprofloxacin	− 8.4	Ser-438, Arg-1122, Asp-1083, Ser-1084, Ala-1120, DG-9, DT-10	Ala-1119, Ala-1120, DG-9	DA-11, Asp-437, Phe-1123, Arg-1122, Met-1121, DT-10

DA = deoxyadenosine; DG = deoxyguanosine; DT = deoxythymidine; DC = Deoxycytidine.

Table 6
Molecular docking results of isolated compounds against Human topoisomerase II β (PDB ID 3QX3)

Compound	Binding Affinity (kcal/mol)	H-bond	Residual interactions	
			Hydrophobic, Electrostatic and others	Van der Waals
1	− 9.2	DG-10, DC-11, Arg-503	DA-12, DG-13 Arg-503	DT-9, Lys-456
2	− 10.1	Glu-477, Asp-557	Tyr-821, Phe-823	Glu-477, Lys-759, His-775, His-774, Gly-776, DT-9, DC-8, Mg-1
3	− 6.4	DG-13, Arg-503, DC-8, Gly-478, Asp-479	Arg-503, Arg-503	DG-10, DT-9, Gly-504, Pro-501, Lys-456
Abiraterone	− 11.8	DG-10	Arg-503, DA-12 DC-8	Gly-504, Glu-477, Gly-478, Lys-456, Asp-479, DT-9
Vosaroxin	− 10.2	Gln-778, DG-10, DG-13, DC-8	DT-9, Arg-503	DA-12, Lys-456, Gly-776

DA = deoxyadenosine; DG = deoxyguanosine; DT = deoxythymidine; DC = Deoxycytidine.

In silico Pharmacokinetics (Drug Likeness) and Toxicity Analysis

The structures of isolated compounds (**1-3**) were converted to their canonical simplified molecular-input lineentry system (SMILE) and submitted to the SwissADME tool to estimate in silico pharmacokinetic parameters (drug-likeness properties) according to 'Lipinski's rule of five [12]. Lipinski's rule of five implies that the drugs and/or candidates should obey the five-parameter rule, which states that hydrogen-bond donors (HBDs) should be less than 5, hydrogen-bond acceptors (HBAs) should be less than 10, molecular mass should be less than 500 Da, log P should not be less than 5, and total polar surface area (TPSA) should not be greater than 140Å. Drug-likeness is a prediction that screens whether a particular organic molecule has properties consistent with being an orally active drug [12]. In the present study, the SwissADME prediction revealed that compounds (**1-3)** obeyed Lipinski's rule of five and they are likely to be orally active (Table 4). The TPSA value of the compounds (**1-3**) was noticed in the range from 20.23 to 57.53 Å and is well below the limit of

140 Å. The calculated numbers of rotatable bonds (NRB) values for the isolated compound (**1-3**) are less than 10(Table 7), which indicated the compounds are conformationally stable.

Table 7
Drug-likeness predictions of compounds, computed by Swiss ADME.

Compound	Mol. Wt. (g/mol)	NHD	NHA	NRB	TPSA ($A^{°2}$)	Log *P* (iLOGP) Lipophilicity	Log *P* (MLOGP) Lipophilicity	Log *S* (ESOL) Water Solubility	Lipinski's rule of five with zero violations
1	316.43	2	3	2	57.53	2.57	3.84	−4.66	0
2	414.71	1	1	6	20.23	4.79	6.73	−7.90	1
3	138.12	2	3	1	57.53	0.85	0.99	−2.07	0
Abiraterone	349.51	1	2	1	33.12	3.42	4.42	−5.03	1
Doxycycline	444.43	6	9	2	181.62	1.11	−2.08	−2.59	1
Vosaroxin	401.45	2	7	5	137.82	2.18	0.19	−2.19	0

NHD = number of hydrogen donors, NHA = number of hydrogen acceptors, NRB = number of rotatable bonds, and TPSA = total polar surface area.

ADMET Properties

The absorption, distribution, metabolism, excretion, and toxicity (ADMET) studies of isolated compounds (**1–3**) were predicted using Swiss ADMET. The skin permeability value (Kp) in cm/s indicates the skin absorption of molecules. In silico, the skin permeability, Kp, values of all compounds ranged from − 2.20 to − 6.02 cm/s suggesting low skin permeability and are within the range of broad-spectrum antibiotic Doxycycline (− 9.03 cm/s) and under the clinical trial anticancer agent Vosaroxin (− 8.98 cm/s). Additionally, gastrointestinal (GI) and blood–brain barrier (BBB) permeation indicate the absorption and distribution of drug molecules. The in-silico prediction results of absorption, distribution, metabolism and excretion (ADME) of the compounds (**1–3**) studied are presented in (Table 8). The Swiss ADME prediction parameters indicated that compound (**1** and **3**) showed high gastrointestinal (GI) absorption, whereas compound (**2**) displayed low absorption and do not showed blood–brain barrier (BBB) permeation. Moreover, a range of cytochromes (CYP's) regulates the drug metabolism, in which CYP1A2, CYP2C19, CYP2C9, CYP2D6, and CYP3A4 are vital for the biotransformation of drug molecules [13]. Thus, in silico SwissADME prediction, only compound (**1**) inhibited cytochrome CYP2C9. However, the compounds (**2** and **3**) are neither cytochromes inhibitor nor a substrate of permeability glycoprotein (P-gp).

Table 8
ADME predictions of compounds, computed by SwissADME and PreADMET.

Compound	Skin Permeation Value (Log *Kp*) cm/s	GI Absorption	BBB Permeability	Inhibitor Interaction					
				Pgp substrate	CYP1A2 inhibitor	CYP2C19 inhibitor	CYP2C9 inhibitor	CYP2D6 inhibitor	CYP3A4 inhibitor
1	−5.08	High	Yes	Yes	No	No	Yes	No	No
2	−2.20	Low	No	No	No	No	No	No	No
3	−6.02	High	Yes	No	No	No	No	No	No
Abiraterone	−5.14	High	Yes	No	Yes	No	No	No	No
Doxycycline	−9.03	Low	No	Yes	No	No	No	No	No
Vosaroxin	−8.98	High	No	Yes	Yes	No	No	No	No

GI = gastrointestinal, BBB = blood brain barrier, P-gp = P-glycoprotein, and CYP = cytochrome-P

Toxicity

Acute toxicity prediction results, such as toxicity class classification and LD_{50} values, predict that all of the isolated compounds (**1–3**) have no acute toxicity. The toxicological prediction gives results of endpoints such as hepatotoxicity, carcinogenicity, mutagenicity, and

cytotoxicity. The studied compounds were predicted to be non- hepatotoxic, non- cytotoxic, non-mutagenic and non-irritant. However, compound (**2**) is Immunotoxic as shown in (Table 9).

Table 9
Toxicity prediction of compounds, computed by ProTox-II and OSIRIS property explorer.

Compound	LD_{50} (mg/kg)	Toxicity Class	Organ Toxicity					
			Hepatotoxicity	Carcinogenicity	Immunotoxicity	Mutagenicity	Cytotoxicity	Irritant
1	5000	5	Inactive	Inactive	Inactive	Inactive	Inactive	No
2	890	4	Inactive	Inactive	Active	Inactive	Inactive	No
3	2200	5	Inactive	Inactive	Inactive	Inactive	Inactive	No
Abiraterone	830	4	Inactive	Inactive	Active	Inactive	Inactive	No
Doxycycline	1007	4	Active	Inactive	Active	Inactive	Inactive	No
Vosaroxin	500	4	Active	Inactive	Inactive	Inactive	Inactive	No

Conclusions

Phytochemical investigation of DCM-MeOH extract of stem bark*P. falcatus*led to the isolation of four compounds 4*β*-carboxy-19-nor-totarol (**1**), β-sitosterol (**2**),*4*-hydroxybenzoic acid (**3**) and (E)-methyl 3, 4, 5-trimethylhex-2-enoate(**4**)and their structures were established on the basis of their ^{1}H and ^{13}C NMR spectral data and comparing with existing literature. Compound **3** is reported for the first time from the genus *Podocarpus*and compound **4** was reported for the first time.The crude extract showed strong activity against *S. aureus*.Whereas, the isolated compounds showed moderate activity against all test strains. The antibacterial activity displayed by the extract support the traditional use of this plant against various ailments caused by bacteria. In silico molecular docking analysis of isolated compounds (**1-3**) against *S. aureus* Gyrase and human DNA topoisomerase IIβ revealed promising scoring pose (lowest energy) with a value ranging from ranging from (−6.1 to −8.6 kcal/mol), with respect to ciprofloxacin and Doxycycline (−8.4 and -13.0 kcal/mol) respectively and ranging from (−6.4 to −10.1 kcal/mol), with respect to Vosaroxin and Abiraterone **(**−10.2 and 11.8 kcal/mol) respectively. Compounds (**1-3**) showed better binding energy (−6.1 to −8.6 kcal/mol) with that of ciprofloxacin (−8.4 kcal/mol), suggesting these compounds could be considered as antibacterial drug lead against *S. aureus*. Compound (**1** and **2**) showed strong binding affinity (−9.2 to −10.1 kcal/mol) with that of vosaroxin (−10.2 kcal/mol) suggesting they can be potential topoisomerase IIβ inhibitors and might be used as anticancer agents. ADMET (drug-likeness) studies showed a good drug-likeness property of all studied compounds, which suggests these compounds, can act as a drug and exhibit remarkable biological activities. The results obtained from molecular docking, drug-likeness properties, ADMET analysis, in good agreement with those obtained from experimental studies suggesting the potential use of the isolated compounds as potential drug leads, which corroborate with the traditional uses of the roots of *P. falcatus*. Further comprehensive evaluations including *invivo* activity tests could be done for conclusive decision on potential candidacy of the plant for formulation and medicinal uses.

Declarations

Conflict of Interests: The authors declare that they have no conflict of interest.

Availability of data and material: NMR data of compounds are available.

Acknowledgements

Mr. Desalegn.A is thankful to Wollega University, Ethiopia for material and financial support for his PhD study.

References

1. Mabberley, David J. The plant-book: a portable dictionary of the vascular plants. Cambridge university press, 1997.
2. Park, H. S., Yoda, N., Fukaya, H., Aoyagi, Y., & Takeya, K. Rakanmakilactones A–F, new cytotoxic sulfur-containing norditerpene dilactones from leaves of Podocarpus macrophyllus var. maki. Tetrahedron, *60*(1), 171–177, 2004.
3. Ito,S. & Kodama, M. Norditerpene dilactones from Podocarpus species. Heterocycles, *4*, 595–624(1976).

4. Aerts,R. Afrocarpus falcatus (Thunb) 2008. http://database.prota.org/PROTAhtml/Afrocarpus%20falcatus En.htm(accessed on July 20, 2020).
5. Lulekal, E., Kelbessa, E., Bekele, T., & Yineger, H. An ethnobotanical study of medicinal plants in Mana Angetu District, south eastern Ethiopia. Journal of Ethnobiology and Ethnomedicine, *4*(1), 1–10(2008).
6. Abdillahi, H. S., Finnie, J. F., & Van Staden, J.(). Anti-inflammatory, antioxidant, anti-tyrosinase and phenolic contents of four Podocarpus species used in traditional medicine in South Africa. Journal of ethnopharmacology, *136*(3), 496–503(2011).
7. Wayne P. A. Performance Standards for Antimicrobial Disc Susceptibility Test, Approved Standard: M02-A11, National Committee for Clinical Laboratory Standards (NCCLS), New York, USA, 11th edition, *32*(1), 1–76. (2012).
8. Nascimento G., Locatelli J., Freitas P., Silva G. Antibacterial activities of plant extracts and phytochemicals on antibiotic resistant Bacteria. Brazilian Journal of Microbiology, 31, 247–256 (2000).
9. Trott, O., Olson, A. J., AutoDock Vina: improving the speed and accuracy of docking with a new scoring function, efficient optimization, and multithreading. J. Comput. Chem., 31, 455–461(2010).
10. Park, H. S., Kai, N., & Fukaya, H. New cytotoxic norditerpene dilactones from leaves of Podocarpus macrophyllus var. maki. Heterocycles, *63*(2), 347–357(2004).
11. Arjun, P., Jha, S., Murthy, P. N., & Manik, A. S. Isolation and characterization of stigmast-5-en-3β-ol (βsitosterol) from the leaves of Hygrophila spinosa T.Anders. International Journal of Pharmaceutical Sciences and Research (IJPSR), 1(2), 95–100 (2010).
12. Lipinski CA, Franco L, Dominy BW, et al. Experimental and computational approaches to estimate solubility and permeability in drug discovery and development settings. Adv Drug Deliv Rev, 23:3–25(1997).
13. Das P, Majumder R, Mahitosh M, et al. In-silico approach for identification of effective and stable inhibitors for COVID-19 main protease (Mpro) from flavonoid based phytochemical constituents of Calendula officinalis. J Biomol Struct Dyn.; 38:1–16 (2020).

Figures

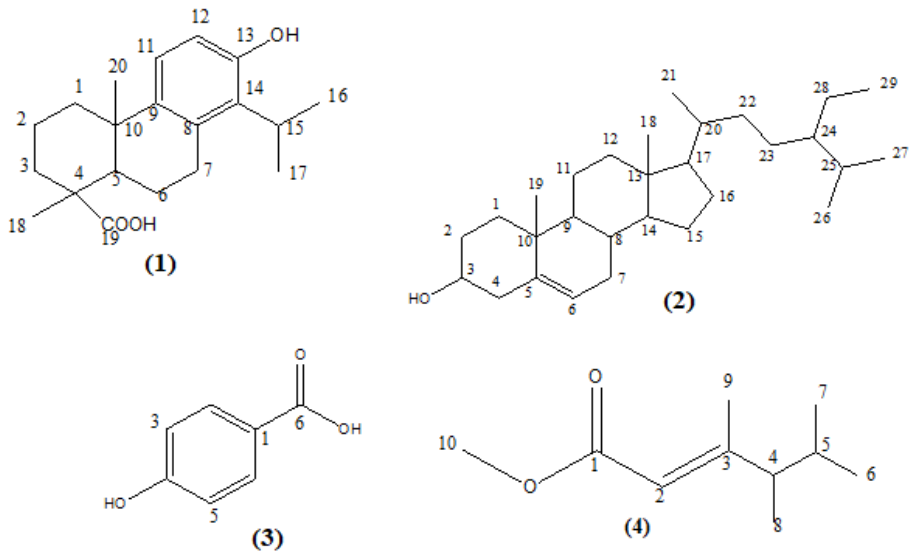

Figure 1

Structure of isolated Compounds from stem bark of *P. falcatus*

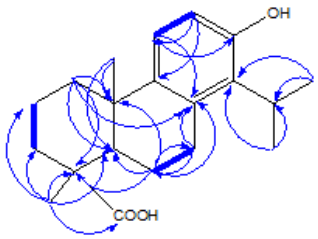

Figure 2

COSY and HMBC correlations of compound 1

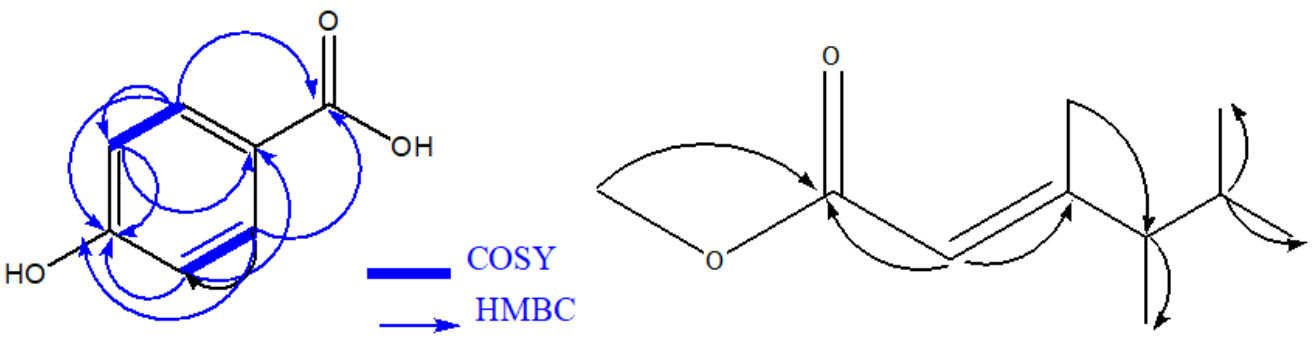

Figure 3

COSY and HMBC correlations of compound **3** and **4**

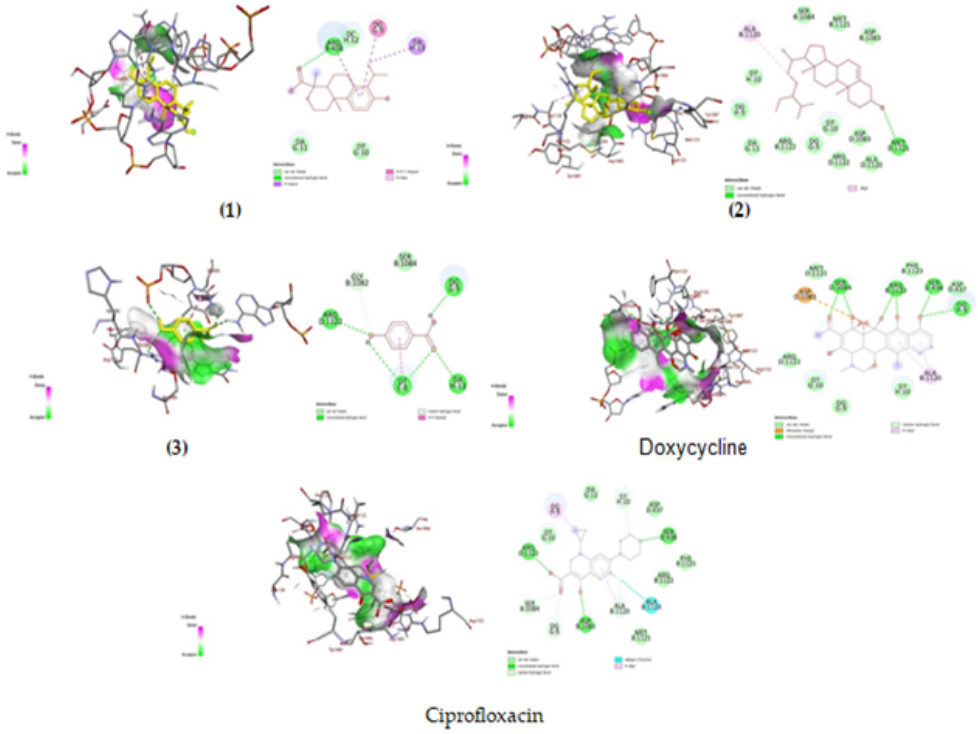

Figure 4

The 2D and 3D binding interactions of compounds (**1-3**) and Reference drugs Doxycycline and Ciprofloxacin against *S. aureus* Gyrase (PDB ID: 2XCT).

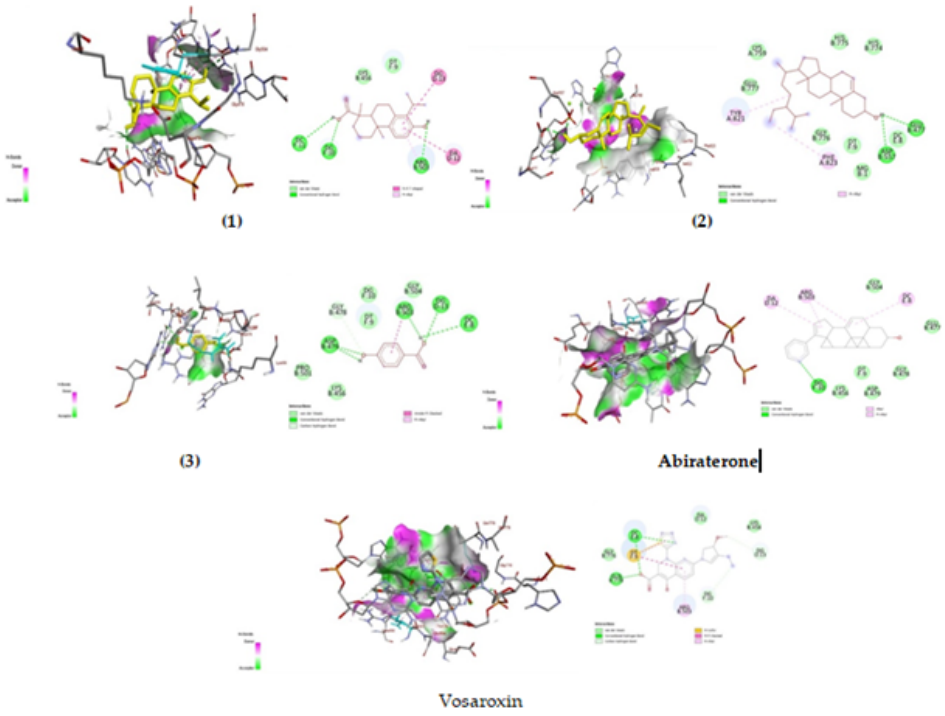

Figure 5

The 2D and 3D binding interactions of compound (**1-3**) and reference drugs Abiraterone and Vosaroxin against human topoisomerase IIβ (PDB ID: 3QX3).

Supplementary Files

This is a list of supplementary files associated with this preprint. Click to download.

- Supplementaryinformation.docx